thermophila β-tubulin-2 gene containing an ATG translation terminator (3′ BTU2) was constructed as in (*10*). A Bluescript KS(+) plasmid (pBS-G8) containing a chromosomal copy of the G8 gene in the middle of a 1.3-kb Sal I–Bam HI fragment was linearized within the G8 coding sequence by digestion with Sty I. The staggered ends were filled in with Klenow, and a Sma I–Eco RV fragment containing the H41-neo-BTU2 chimeric gene was ligated into the linearized pBS-G8 plasmid. The resulting plasmid, pG8-neo, was digested with Sal I and Bam HI liberating a 2.7-kb fragment containing the disrupted G8 gene and its normal flanking sequences. This DNA was used to transform, by electroporation, the *T. thermophila* strain CU427 (*11*). Transformants were initially selected with paromomycin (120 μg/ml) in the growth medium. Further selection in higher concentrations of paromomycin (up to 750 μg/ml) produced cell lines that remained resistant to a concentration of paromomycin of 750 μg/ml even when grown for 30 to 40 generations in the absence of drug. These lines were designated G8 null cells. BTU2 null cells are a strain of *T. thermophila* developed in the Gorovsky lab in which the β-tubulin-2 gene contains a *neo* insertion. They are otherwise isogenic with CU427 and G8 null cells.

14. R. L. Hallberg and E. M. Hallberg, *Mol. Cell. Biol.* **3**, 502 (1983).
15. R. L. Hallberg *et al.*, *ibid.* **5**, 2061 (1985).
16. R. L. Hallberg, *ibid.* **6**, 2267 (1986).
17. E. M. Hallberg and R. L. Hallberg, unpublished data. Cultures of early log phase G8 null and CU427 cells at 30°C were either maintained at that temperature or were shifted to 39°C for 1 hour. All cultures were then transferred to 46°C, and at 3-min intervals thereafter (for a total of 12 min), samples of cells were removed from each culture; individual cells from each sample were then transferred to growth medium in microtiter plates and incubated at 30°C. Twenty-four hours later, the fraction of viable cells was determined. Both G8 null and CU427 cells given a 1-hour prior heat shock exhibited a degree of thermotolerance similar to that shown for a number of other strains (*15, 18*).
18. K. W. Kraus, E. M. Hallberg, R. L. Hallberg, *Mol. Cell. Biol.* **6**, 3854 (1986).
19. R. L. Hallberg *et al.*, *Cell* **26**, 47 (1981).

20. From individual cultures of cells in starvation medium at 43°C, 0.2-ml samples were removed at various times and added to 0.05 ml of prewarmed starvation medium containing [^{3}H]lysine (100 μCi/ml). Incubation was continued at 43°C for 10 min, after which triplicate 75-μl samples were removed and trichloroacetic acid (TCA) added to 10%. The insoluble material was collected on filters, washed, dried, and counted. This TCA-insoluble incorporation was used as an estimate of the rate of protein synthesis. The values plotted are calculated from the means of the counts per minute in the three samples collected.

21. We thank E. M. Hallberg for her expert technical assistance in carrying out the thermotolerance experiments. This work was supported by NIH grants GM46302 (to R.L.H.) and GM26973 (to M.A.G.).

27 October 1994; accepted 14 February 1995

Structure of a Complex of Two Plasma Proteins: Transthyretin and Retinol-Binding Protein

Hugo L. Monaco,* Menico Rizzi, Alessandro Coda

The three-dimensional structure of the complex formed by two plasma proteins, transthyretin and retinol-binding protein, was determined from x-ray diffraction data to a nominal resolution of 3.1 angstroms. One tetramer of transthyretin was bound to two molecules of retinol-binding protein. The two retinol-binding protein molecules established molecular interactions with the same transthyretin dimer, and each also made contacts with one of the other two monomers. Thus, the other two potential binding sites in a transthyretin tetramer were blocked. The amino acid residues of the retinol-binding protein that were involved in the contacts were close to the retinol-binding site.

Transthyretin (TTR, formerly called prealbumin), one of the transporters of the hormone thyroxine, and retinol-binding protein (RBP), the specific carrier of retinol (vitamin A), form a complex under physiological conditions that prevents the glomerular filtration of the low molecular size RBP (21,000 daltons) in the kidneys (*1*). The complex can form in vitro between RBP and TTR from different species, including those species that are distant in evolution (*2*). We prepared crystals from complexes containing human TTR and chicken RBP (*3*). The dissociation constant of this complex (1.0×10^{-7} M) is similar to those of the complexes of human RBP with human TTR (1.1×10^{-7} to 1.5×10^{-7} M) and of chicken RBP with chicken TTR (1.1×10^{-7} to 1.6×10^{-7} M) (*4*).

The crystallographic data of this complex are presented in Table 1. The structure of the complex was solved with the molecular replacement method (*5*) with one of the human TTR coordinate sets (*6*) and coordinates of bovine holo-RBP (*7*). The final model statistics (*8*) are an *R* factor of 20.1 (*R* factor $= \Sigma \mid F_o - F_c \mid / \Sigma \mid F_o \mid$ where F_o is the observed and F_c the calculated structure factor) with root-mean-square deviations in the bonds of 0.018 Å, in the angles of 3.7°, and in the dihedrals of 26.7°.

Department of Genetics, University of Pavia, 27100 Pavia, Italy.

*To whom correspondence should be addressed.

The three-dimensional structure of human (*9*, *10*) and bovine (*7*) holo- and apo-RBP, of wild-type (*11*) and several mutant human TTRs (*12*, *13*), and of complexes of wild-type TTR with several pharmacologically important compounds (*6*, *14*) are all known. TTR is a tetramer of four identical subunits, each 127 amino acids long (Fig. 1) (*11*). The monomers are organized into two extensive β sheets, each composed of four strands that are all antiparallel, with one exception (*11*). Two monomers form a stable dimer by the extension of their two β sheets through hydrogen bonding that involves the four strands (two from each monomer) at the edges of the two subunits. The two dimers of the tetramer are separated by a channel and in contact through symmetry related loops. The channel, approximately 10 Å in diameter, is the ligand-binding site

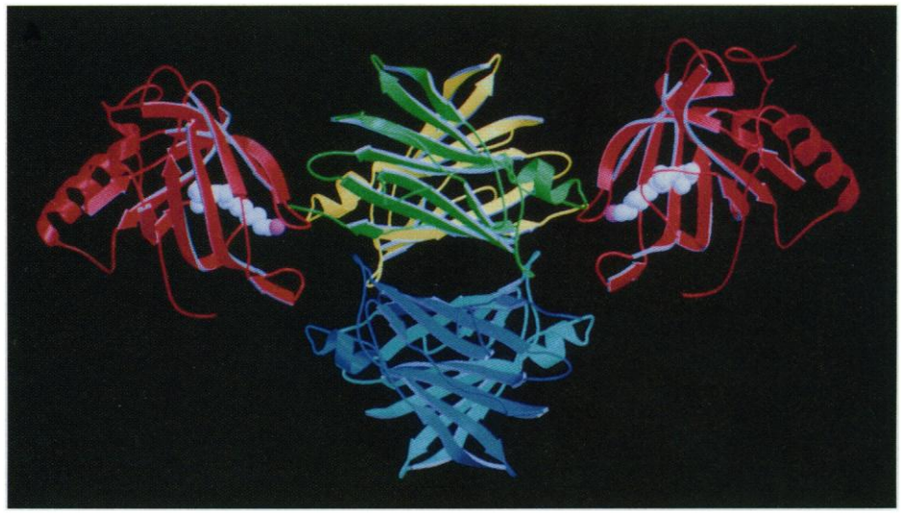

Fig. 1. Model of the structure of the hexameric complex $(RBP)_2$-TTR as determined by x-ray analysis of the orthorhombic crystals. The RBP molecules are shown in red, one of the TTR dimers is in green and yellow, and the other is in blue and turquoise. The retinol molecules are represented as space-filling models with white carbon atoms and a purple oxygen. The view is looking down the *z* axis of the TTR tetramer as defined by Blake and co-workers (*11*). The *x* and *y* axes are in the plane of the figure, horizontally and vertically, respectively. They intercept in the center of the channel, which is the hormone-binding site, that runs through the TTR tetramer and is empty in the figure.

(*11*). The three orthogonal molecular twofold axes of TTR have been designated *x*, *y*, and *z*, the latter being coincident with the ligand-binding channel of the molecule (*11*).

The RBP molecule is shaped like a calix made up of eight strands of antiparallel β sheets that are followed topologically by a short α-helical segment (*9*). Into this calix, the retinol molecule binds with the β-ionone ring buried the deepest and with the alcohol moiety pointing to the outside on the surface of the molecule. The presence of the vitamin bound to RBP is essential for the formation of a stable complex with TTR (*15*). After removal of retinol, the complex dissociates and the low molecular size apo-RBP can be filtered in the kidneys (*1*). The transition from holo- to apoprotein of human and bovine RBP involves a conformational change on the loop extending from amino acids 34 to 37, in particular in Leu[35] and Phe[36] (*7*, *10*). The space vacated by the removal of the vitamin is filled in both cases by solvent molecules and the aromatic ring of Phe[36].

The crystallographic asymmetric unit of the complex contained one TTR tetramer plus two RBP molecules. In this hexamer, the TTR *y* axis was preserved, whereas the two RBP molecules bound to the tetramer along an axis that was parallel to the TTR *x* axis (Fig. 1) and that was close enough to it to hinder the potential binding of two other RBP molecules that would be required to satisfy this symmetry element in an octameric complex. Thus, this structure establishes the stoichiometry of the complex as a maximum of two RBP molecules per TTR tetramer (*15*, *16*). The binding of either of the two RBP molecules precluded the possibility that the TTR *x* axis could be preserved in the hexamer, but why it was the *y* axis and not the *z* axis that was present in the complex was not evident.

Table 1. Crystallographic data. The crystals were orthorhombic, space group *I*222 with a = 222.4 Å, b = 163.4 Å, and c = 55.5 Å. The data were collected and a Rigaku *R*-axis II imaging plate detector and a Rigaku RU-200 source (Molecular Structure, The Woodlands, Texas). The frame size was 1.5°, and the exposure time was 50 min per frame. There were 47,491 observations up to a 3.1 Å resolution with 17,465 unique reflections. The data set was 94.8% complete and had an R_{sym} = 0.090. All the reflections recorded were kept in the file. FSQ is the square of the structure factor and sig is the standard deviation.

Resolution (Å)	<FSQ/sig>	Reflections	% in interval	Cumulative (%)
6.0–5.0	13.75	1847	97.3	95.9
5.0–4.0	11.07	4185	98.6	97.2
4.0–3.5	4.78	4140	97.3	97.2
3.5–3.3	3.06	2360	95.2	96.9
3.3–3.1	2.06	2359	83.2	94.8

Table 2. Significant contacts in the RBP-TTR complex. The RBP molecule selected is chain E. Chains A and B listed under TTR are from the two subunits of one of the TTR dimers, and chain C is a TTR monomer from the other dimer. The designations in the brackets refer to the particular atom involved in the interaction.

RBP residue	Distance (Å)	TTR residue
Leu[35][CD2]	3.41	B-Gly[83][CA]
Trp[67][CZ2]	4.20	C-Val[20][CG1]
Trp[67][CD2]	3.45	C-Ile[84][CD1]
Lys[89][NZ]	2.73	A-Asp[99][CO]
Lys[89][NZ]	4.54	A-Asp[99][OD2]
Trp[91][NE1]	4.07	A-Ser[100][CO]
Ser[95][CO]	3.03	B-Tyr[114][OH]
Phe[96][CO]	2.69	B-Ser[85][N]
Phe[96][N]	3.38	B-Tyr[114][OH]
Phe[96][CB]	3.37	B-Ile[84][CG2]
Phe[96][CE1]	3.44	C-Arg[21][CG]
Leu[97][CO]	2.80	B-Ser[85][OG]
Lys[99][NZ]	2.70	A-Asp[99][OD2]
Lys[99][N]	3.87	B-Ser[85][OG]
Retinol[OH]	3.15	B-Gly[83][CO]

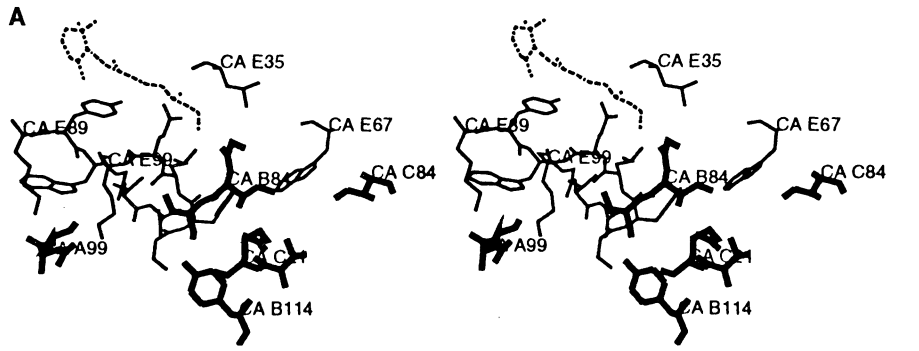

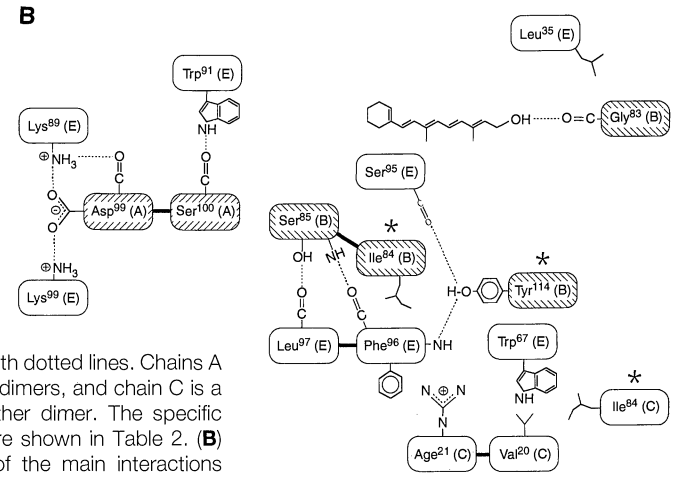

Fig. 2. (**A**) Stereo diagram showing the amino acids interacting from one of the RBP molecules (chain E of RBP, drawn with thinner lines) with the three TTR monomers in contact with it (drawn with thicker lines). CA refers to the α carbons, and the single letter followed by a number indicates the chain and amino acid position, respectively. The retinol molecule has been drawn with dotted lines. Chains A and B form one of the TTR dimers, and chain C is a TTR monomer from the other dimer. The specific residues and interactions are shown in Table 2. (**B**) Schematic representation of the main interactions shown in (A). The letter in parentheses specifies the chain. An asterisk identifies TTR amino acids whose mutations have been described in the medical literature. Retinol is shown linked to Gly[83] on chain B.

Fig. 3. Comparison of the amino acid sequences of (**A**) RBP (*25*) and (**B**) TTR (*26*) from different species. Numbering of the residues corresponds to the sequences of bovine RBP and human TTR. The boxed amino acids are involved in the interactions between the two macromolecules. Abbreviations for the amino acid residues are as follows: A, Ala; C, Cys; D, Asp; E, Glu; F, Phe; G, Gly; H, His; I, Ile; K, Lys; L, Leu; M, Met; N, Asn; P, Pro; Q, Gln; R, Arg; S, Ser; T, Thr; V, Val; W, Trp; and Y, Tyr.

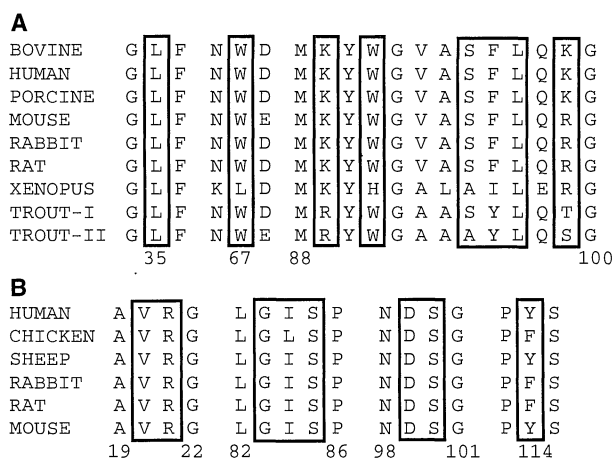

This observation may have been related to the packing of the molecules in this crystal form.

Out of the total RBP surface accessible to the solvent (9356 Å^2), 736 Å^2 (about 8%) was buried when in contact with TTR (*17*). The main residues in contact in the complex are listed in Table 2. Isoleucines at position 84 from two different chains of TTR participated in the interactions with each of the RBP molecules, and the retinol hydroxyl group was within hydrogen bonding distance of the peptide carbonyl of the same TTR Gly (position 83) that interacts with RBP Leu^{35} and that plays a role in the holo to apo transition (*7*, *10*).

Many experimental observations can be explained by this x-ray structure (*18*). Complex formation is known to stabilize the binding of retinol to RBP, and substitution of this ligand can impair or even prevent the interaction of the two macromolecules. This agrees with the observation that the retinol hydroxyl group was found to participate in the contacts with TTR (Fig. 2). The binding of thyroxine to TTR is identical in the complex to the binding in the isolated macromolecule (*19*), which is compatible with the fact that the ligand-binding site is located in an area that did not participate in any way in the macromolecular interactions (*11*). At least one Lys and a Trp residue of RBP are believed to be present in the area that interacts with TTR (*20*). Our structure showed that lysines 89 and 99 and tryptophans 67 and 91 of RBP were part of the surface in contact with TTR (Fig. 2). In addition, the role of Leu^{35} in the holo to apo transition of RBP, which results in a change in affinity for TTR, was also clarified by this structure (Fig. 2).

The amino acid residues of RBP and TTR that are involved in the contacts in the complex have been identified (Fig. 3). In most cases, the contact sites were found in conserved regions, which explains the cross-reactivity between RBP and TTR from distant species.

More than 40 pathological variants of human TTR have been described (*21*). They are mostly associated with familial amyloidotic polyneuropathy (*21*) but also with senile systemic amyloidosis (*22*) and euthyroid hyperthyroxinemia (*13*). In two of these mutants, the altered residues (*23*) would be involved in the interactions with RBP. In individuals with the mutation Ile^{84} → Ser, the presence of the altered gene correlated with lower concentrations of serum RBP (*24*).

The extent and types of interactions between amino acids revealed by this structure are not dissimilar to those observed in other protein-protein complexes. Our findings explain the role played by retinol in the relative stability of the RBP-TTR complex.

REFERENCES AND NOTES

1. M. Kanai, A. Raz, D. W. S. Goodman, *J. Clin. Invest.* **47**, 2025 (1968); P. A. Peterson, *J. Biol. Chem.* **246**, 44 (1971); D. W. S. Goodman, in *The Retinoids*, M. B. Sporn, A. B. Roberts, D. W. S. Goodman, Eds. (Academic Press, New York, 1984), vol. 2, pp. 41–88.
2. L. Rask, *Eur. J. Biochem.* **44**, 1 (1974).
3. H. L. Monaco, F. Mancia, M. Rizzi, A. Coda, *J. Mol. Biol.* **244**, 110 (1994). The crystals were grown with the proteins in a ratio of two molecules of RBP per TTR tetramer. The normal RBP concentration in human plasma is about 2 mM and that of TTR about 4.5 mM. Therefore, the stoichiometry of the predominant complex in vivo is believed to be one molecule of RBP per TTR tetramer. In addition to the orthorhombic crystals whose structure is described here, a tetragonal form was found for complexes formed by the proteins purified from other species. The tetragonal crystals did not diffract to a high enough resolution, and their space group could not be determined beyond doubt because some systematic absences were difficult to establish. The space group was probably $P4_12_12$ with a = 142.2 Å and c = 124.4 Å. The highest number of reflections of this crystal form that we were able to collect was significantly lower than the number used in this study.
4. M. Kopelman, U. Cogan, S. Mokady, M. Shinitzky, *Biochim. Biophys. Acta* **439**, 449 (1976).
5. The calculations were performed with the AMoRe package [J. Navaza, *Acta Crystallogr.* **A50**, 157 (1994)]. When the rotation function was calculated with a TTR dimer as search probe, two peaks related by a 180° rotation were found with correlation coefficients of 19.4 and 19.2. If the rotation function was calculated with a TTR tetramer instead, the two peaks had correlation coefficients of 28.3 and 28.2. When the rotation function was calculated with bovine RBP as search probe, two major peaks with correlation coefficients of 21.7 and 18.4 were found (the third peak had a correlation coefficient of 14.7). The translation function of the rotated TTR tetramer gave a solution with a correlation coefficient of 27.5 and an R factor of 46.9 if the space group $I222$ was assumed, and a correlation coefficient of 10.5 and an R factor of 54.5 if the enantiomeric space group $I2_12_12_1$ was assumed instead. When the translation function was calculated with the RBP molecule rotated according to the first solution found, the solution had a correlation coefficient of 17.9 and an R factor of 48.3 if the space group assumed was $I222$ and 12.2 and 49.3, respectively, if the enantiomeric space group $I2_12_12_1$ was assumed instead. At this point, we checked the molecular packing in order to select the correct space group. Of the two possible enantiomeric space groups, only $I222$ did not cause clashing of the molecules in the unit cell and therefore $I2_12_12_1$ was discarded. The pentamer was assembled and rigid body refined. This was followed by Powell refinement with the X-PLOR package imposing noncrystallographic symmetry [A. T. Brünger, *X-PLOR: A System for Crystallography and NMR, 3.1 Manual* (Yale Univ. Press, New Haven, CT, 1992)]. After this operation, the R factor was 31.9, and the model had reasonable geometry. A $2F_o - F_c$ map was calculated (F_o is the observed and F_c is the calculated structure factor), and we found enough electron density to fit a second RBP molecule. The two RBPs satisfied the TTR y twofold axis. The hexamer was assembled, and no molecular clashings were observed in the unit cell. When this model underwent rigid body and Powell refinement imposing noncrystallographic symmetry, the R factor dropped to 24.4, and the geometry remained reasonable. When an electron density map was examined, it was found there was electron density for the retinol and thyroxine molecules that had not been included in the model. The model was rebuilt and some side chains were repositioned, then it was Powell refined imposing noncrystallographic symmetry. In the last cycle, two temperature factors per residue were used.
6. A. Wojtczak, J. R. Luft, V. Cody, *J. Biol. Chem.* **268**, 6202 (1993).
7. G. Zanotti, R. Berni, H. L. Monaco, *ibid.*, p. 10728.
8. Refinement was done with the reflections in the resolution range of 6.0 to 3.1 Å. The final model contained 6624 nonhydrogen atoms and no water molecules.
9. S. W. Cowan, M. E. Newcomer, T. A. Jones, *Proteins Struct. Funct. Genet.* **8**, 44 (1990).
10. G. Zanotti, S. Ottonello, R. Berni, H. L. Monaco, *J. Mol. Biol.* **230**, 613 (1993).
11. C. C. F. Blake, M. J. Geisow, I. D. A. Swan, C. Rérat, B. Rérat, *ibid.* **88**, 1 (1974); C. C. F. Blake and S. J. Oatley, *Nature* **268**, 115 (1977); C. C. F. Blake, M. J. Geisow, S. J. Oatley, B. Rérat, C. Rérat, *J. Mol. Biol.* **121**, 339 (1978).
12. C. J. Terry *et al.*, *EMBO J.* **12**, 735 (1993); J. A. Hamilton *et al.*, *J. Biol. Chem.* **268**, 2416 (1993).
13. L. K. Steinrauf, J. A. Hamilton, B. C. Braden, J. R. Murrell, M. D. Benson, *J. Biol. Chem.* **268**, 2425 (1993).
14. E. Ciszak, V. Cody, J. R. Luft, *Proc. Natl. Acad. Sci. U.S.A.* **89**, 6644 (1992); A. Wojtczak, J. R. Luft, V. Cody, *J. Biol. Chem.* **267**, 353 (1992).
15. N. Noy, E. Slosberg, S. Scarlata, *Biochemistry* **31**, 11118 (1992).
16. P. P. van Jaarsveld, H. Edelhoch, D. S. Goodman, J. Robins, *J. Biol. Chem.* **248**, 4698 (1973); L. Trägårdh, H. Anundi, L. Rask, K. Sege, P. A. Peterson, *ibid.* **255**, 9243 (1980).
17. This figure can be compared with the 748 Å^2, which are 11% of the total accessible surface, of lysozyme that are buried in one of the lysozyme-antibody complexes [R. A. Mariuzza, S. E. V. Phillips, R. J. Poljak, *Annu. Rev. Biophys. Chem.* **16**, 139 (1987)].
18. J. Åqvist and O. Tapia [*J. Mol. Graphics* **10**, 120 (1992)] have proposed a model for this complex based on computer graphics docking simulations with the known three-dimensional structures of the two proteins. Their model explained many experimental observations available at the time (reviewed in their paper), but the subsequent results on the structures of holo- and apo-RBP cannot be explained by it. Although some of the residues involved in the contacts were correctly identified, their theoretical model is different from the x-ray structure presented here.
19. A. Raz and D. S. Goodman, *J. Biol. Chem.* **244**, 3230 (1969).
20. H. Horwitz and J. Heller, *ibid.* **249**, 7181 (1974); J. Heller and H. Horwitz, *ibid.* **250**, 3019 (1975).
21. M. D. Benson, in *The Metabolic Basis of Inherited Disease*, C. R. Scriver, A. L. Beaudet, W. S. Sly, D. Valle, Eds. (McGraw-Hill, New York, ed. 7, 1993), pp. 6262–6310.
22. D. R. Jacobson, P. D. Gorevic, J. N. Buxbaum, *Am. J. Hum. Genet.* **47**, 127 (1990).
23. S. Ueno, T. Uemichi, S. Yorifuji, S. Tarui, *Biochem. Biophys. Res. Commun.* **169**, 143 (1990); M. R. Wallace, P. M. Conneally, M. D. Benson, *Am. J. Hum. Genet.* **43**, 182 (1988).
24. M. D. Benson and F. E. Dwulet, *Arthritis Rheum.* **26**, 1493 (1983). This result has been confirmed by the work of R. Berni *et al.* [*J. Biol. Chem.* **269**, 23395 (1994)]. Using the fluorescence anisotropy of the retinol bound to RBP, they found that the affinity of the Ser^{84} TTR mutant for normal human RBP is negligible.
25. R. Berni *et al.*, *Eur. J. Biochem.* **192**, 507 (1990); L. Rask, H. Anundi, P. A. Peterson, *FEBS Lett.* **104**, 55 (1979); J. Sundelin *et al.*, *J. Biol. Chem.* **260**, 6472 (1985); M. C. Zapponi, G. Zanotti, M. Stoppini, R. Berni, *Eur. J. Biochem.* **210**, 937 (1992).
26. W. Duan *et al.*, *Eur. J. Biochem.* **200**, 679 (1991).

27. We thank M. Amzel, F. Mancia, A. Mattevi, and G. L. Rossi for discussions. Supported by grants from the Italian National Research Council and the Ministry of the Universities and Scientific Research. Coordinates have been deposited in the Brookhaven Protein Data Bank under the identity code 1RLB.

19 December 1994; accepted 3 March 1995